AMERICAN SOCIETY FOR MICROBIOLOGY | Antimicrobial Agents and Chemotherapy®

PHARMACOLOGY

# Population Pharmacokinetics and Dosing of Ethionamide in Children with Tuberculosis

Henrik Bjugård Nyberg,[a] Heather R. Draper,[b] Anthony J. Garcia-Prats,[b] Stephanie Thee,[c] Adrie Bekker,[b] Heather J. Zar,[d,e] Andrew C. Hooker,[a] H. Simon Schaaf,[b] Helen McIlleron,[f] Anneke C. Hesseling,[b] Paolo Denti[f]

[a]Department of Pharmaceutical Biosciences, Uppsala University, Uppsala, Sweden
[b]Desmond Tutu TB Centre, Department of Paediatrics and Child Health, Faculty of Medicine and Health Sciences, Stellenbosch University, Cape Town, South Africa
[c]Department of Pediatrics, Division of Pneumonology, Immunology and Intensive Care, Charité University Medicine, Berlin, Germany
[d]Department of Paediatrics and Child Health, Red Cross War Memorial Children's Hospital, Cape Town, South Africa
[e]MRC Unit on Child & Adolescent Health, University of Cape Town, Cape Town, South Africa
[f]Division of Clinical Pharmacology, Department of Medicine, University of Cape Town, Cape Town, South Africa

**ABSTRACT** Ethionamide has proven efficacy against both drug-susceptible and some drug-resistant strains of *Mycobacterium tuberculosis*. Limited information on its pharmacokinetics in children is available, and current doses are extrapolated from weight-based adult doses. Pediatric doses based on more robust evidence are expected to improve antituberculosis treatment, especially in small children. In this analysis, ethionamide concentrations in children from 2 observational clinical studies conducted in Cape Town, South Africa, were pooled. All children received ethionamide once daily at a weight-based dose of approximately 20 mg/kg of body weight (range, 10.4 to 25.3 mg/kg) in combination with other first- or second-line antituberculosis medications and with antiretroviral therapy in cases of HIV coinfection. Pharmacokinetic parameters were estimated using nonlinear mixed-effects modeling. The MDR-PK1 study contributed data for 110 children on treatment for multidrug-resistant tuberculosis, while the DATiC study contributed data for 9 children treated for drug-susceptible tuberculosis. The median age of the children in the studies combined was 2.6 years (range, 0.23 to 15 years), and the median weight was 12.5 kg (range, 2.5 to 66 kg). A one-compartment, transit absorption model with first-order elimination best described ethionamide pharmacokinetics in children. Allometric scaling of clearance (typical value, 8.88 liters/h), the volume of distribution (typical value, 21.4 liters), and maturation of clearance and absorption improved the model fit. HIV coinfection decreased the ethionamide bioavailability by 22%, rifampin coadministration increased clearance by 16%, and ethionamide administration by use of a nasogastric tube increased the rate, but the not extent, of absorption. The developed model was used to predict pediatric doses achieving the same drug exposure achieved in 50- to 70-kg adults receiving 750-mg once-daily dosing. Based on model predictions, we recommend a weight-banded pediatric dosing scheme using scored 125-mg tablets.

**KEYWORDS** ethionamide, multidrug resistance, pediatric infectious disease, population pharmacokinetics, tuberculosis

Approximately 1 million children develop tuberculosis (TB) disease every year, with 32,000 children being estimated to have multidrug-resistant TB (MDR-TB) (1). As MDR-TB becomes more prevalent, improved knowledge of drugs beyond those used for first-line treatment is increasingly important. Ethionamide is an older drug with proven efficacy against *Mycobacterium tuberculosis* (2) and is now a group C second-line anti-TB drug to be used when an effective regimen cannot otherwise be constructed (2,

**Citation** Bjugård Nyberg H, Draper HR, Garcia-Prats AJ, Thee S, Bekker A, Zar HJ, Hooker AC, Schaaf HS, McIlleron H, Hesseling AC, Denti P. 2020. Population pharmacokinetics and dosing of ethionamide in children with tuberculosis. Antimicrob Agents Chemother 64:e01984-19. https://doi.org/10.1128/AAC.01984-19.



Address correspondence to Paolo Denti, paolo.denti@uct.ac.za.

**Received** 1 October 2019
**Returned for modification** 29 October 2019
**Accepted** 12 December 2019
**Accepted manuscript posted online** 23 December 2019
**Published** 21 February 2020

3). It is also used as part of first-line treatment in some situations, such as in TB meningitis, due to its ability to cross the blood-brain barrier (4, 5), or in small children requiring a fourth drug when suitable formulations of ethambutol are not available (6).

Ethionamide treatment is associated with frequent adverse events. Similar to other thioamides, it is known to cause gastrointestinal intolerance, hepatotoxicity, hypothyroidism, peripheral neuropathy, and psychiatric adverse effects, including sleep disorders (7, 8). Gastrointestinal intolerance may lead to reduced adherence and complicate oral administration in patients regularly taking a large number of drugs (9). Defining optimal dosing is therefore important.

The current South African pediatric dosing guidelines advise that ethionamide be used at 15 to 20 mg/kg of body weight in patients with MDR-TB and 20 mg/kg in patients with miliary TB or TB meningitis (10). A weight-banded regimen has recently been suggested by WHO (11). Both recommendations are mostly based on extrapolations from the adult dose, but the current understanding of ethionamide pharmacokinetics is limited, especially in children and infants.

Our aim was to characterize the pharmacokinetics of ethionamide in children with tuberculosis, identifying and quantifying relevant factors affecting drug concentrations, and to evaluate whether the dosing guidelines achieve pediatric drug exposures in line with expected adult values.

## RESULTS

**Study population and pharmacokinetic samples.** A total of 119 children were included in the analysis; 110 were from the MDR-PK1 study (9) and 9 were from the DATiC study (30, 31), with 4 children undergoing repeated pharmacokinetic sampling visits, giving a total of 730 samples in 124 ethionamide concentration profiles, 2 of which were partial. Concentrations were below the lower limit of quantitation (BLQ) in 15% of the samples, and all but one of these was predose. The median age of the children in the cohort was 2.6 years (range, 3 months to 15 years), and the median weight was 12.5 kg (range, 2.5 to 66 kg). Coinfection with HIV was present in 24 children, 20 of whom were on antiretroviral therapy (ART) based on either lopinavir-ritonavir ($n = 14$) or efavirenz ($n = 6$). An overview of participant characteristics is shown in Table 1.

**Population pharmacokinetic model.** Ethionamide pharmacokinetics were well described using a one-compartment disposition model with first-order elimination and a transit compartment (12) absorption (Fig. 1). The parameter estimates are shown in Table 2, and the NONMEM model code is provided in the supplemental material.

Allometric scaling to body weight (13, 40) was applied to clearance (CL) (change in the objective function value [ΔOFV] = 34.8) and volume of distribution ($V$) (ΔOFV = 120.2), with body weight being a better body size descriptor than fat-free mass. After allometry, maturation of clearance was included in the model (ΔOFV = 22.4, $P = 1.4 \times 10^{-5}$). The model predicted that clearance maturation would reach 50% within 2 months after birth and >95% maturity at about 2 years of age, as shown in Fig. S1 in the supplemental material.

Administration using a nasogastric tube (NGT) increased the speed of absorption by shortening the absorption mean transit time (MTT) (ΔOFV = 21.8, $P = 3.0 \times 10^{-6}$). HIV coinfection was found to lower the bioavailability and, thus, exposure by 22% (ΔOFV = 14.5, $P = 1.4 \times 10^{-4}$). Rifampin cotreatment increased clearance by 16% (ΔOFV = 7.1, $P = 7.7 \times 10^{-3}$).

The absorption rate constant ($k_a$) and MTT were found to be faster in smaller children (ΔOFV = 16.4, $P \leq 5.1 \times 10^{-5}$). This was best captured using the exponential maturation function shown in equations 1 and 2.

$$k_{a,i} = k_{a,\mathrm{std}} \cdot \left[1 + \left(\mathrm{Scale}_{\mathrm{Abs}} - 1\right) \cdot e^{-\gamma_{\mathrm{mat,Abs}} \cdot \mathrm{Age}_i}\right] \quad (1)$$

$$\mathrm{MTT}_i = \frac{\mathrm{MTT}_{\mathrm{std}}}{\left[1 + \left(\mathrm{Scale}_{\mathrm{Abs}} - 1\right) \cdot e^{-\gamma_{\mathrm{mat,Abs}} \cdot \mathrm{Age}_i}\right]} \quad (2)$$

where the subscript $i$ denotes values for patient $i$, std denotes fully mature values,

**TABLE 1** Characteristics of study populations treated with antituberculosis regimens including ethionamide

| Characteristic | Value for the following study population: | | |
|---|---|---|---|
| | MDR-PK1 | DATiC | Pooled data |
| No. (%) of children of the following ethnicity: | | | |
| Black | 65 (59.1) | 7 (77.8) | 72 (60.5) |
| Mixed race | 45 (40.9) | 2 (22.2) | 47 (39.5) |
| No. (%) of male children | 58 (52.7) | 6 (66.7) | 64 (53.7) |
| Median (range) age (yr) | 3.0 (0.46 to 15) | 0.7 (0.23 to 2.3) | 2.6 (0.23 to 15) |
| Median (range) wt (kg) | 13 (6.0 to 66) | 6.1 (2.5 to 14) | 12.5 (2.5 to 66) |
| Median (range) WHO Z-score for: | | | |
| Wt for age ($n$ = 109)[a] | −0.64 (−4.77 to 1.99) | −2.35 (−5.57 to 0.83) | −0.64 (−5.57 to 1.99) |
| Ht for age | −1.61 (−4.70 to 1.43) | −2.66 (−5.94 to −1.04) | −1.71 (−5.94 to 1.43) |
| BMI[b] for age | 0.33 (−3.82 to 4.16) | 1.48 (−4.95 to 2.58) | 0.34 (−4.95 to 4.16) |
| Median (range) ethionamide total dose (mg) | 264 (120 to 1,000) | 125 (50 to 250) | 250 (50 to 1,000) |
| Median (range) ethionamide dose (mg/kg) | 20.0 (10.4 to 24.7) | 20.5 (16.0 to 25.3) | 20.0 (10.4 to 25.3) |
| No. (%) of patients receiving ethionamide: | | | |
| As a whole tablet orally | 18 (16.4) | 0 (0) | 18 (15.1) |
| As a crushed tablet orally | 17 (15.5) | 2 (22.2) | 19 (16.0) |
| As a crushed tablet via NGT | 75 (68.1) | 7 (77.8) | 82 (68.9) |
| Coadministered with rifampin | 12 (10.9) | 9 (100) | 21 (17.6) |
| No. (%) of patients with HIV coinfection | 23 (20.9) | 1 (11.1) | 24 (20.2) |

[a]WHO weight-for-age Z-scores are defined only for ages up to 10 years. Ten subjects over 10 years of age were therefore not assigned a value and were not used to estimate a weight-for-age effect in the covariate search.
[b]BMI, body mass index.

$Scale_{Abs}$ is the scaling factor for maturation of absorption, meaning the relative change in the parameter value (expressed in fold) for a child at birth, and $\gamma_{mat,Abs}$ is the shape factor for maturation of absorption, meaning the exponential rate at which the effect reaches the mature values. Absorption was estimated to be 2.43-fold faster at birth, with the effect waning at about 3 years of age ($\gamma_{mat,Abs}$ was fixed to 1/year to stabilize the model), as shown in Fig. S1.

The best statistical model included interoccasion variability (IOV) on bioavailability, MTT, and $k_a$, as well as interindividual variability (IIV) on clearance. IIV on the volume of distribution was not supported by the data and could not be robustly estimated.

While the predose concentrations in most patients were BLQ (and were imputed to the lower limit of quantitation [LLOQ]/2), 15 unexpectedly high predose values were observed. The pharmacokinetic profiles observed in these patients after the dose administered at the clinic were in line with those observed in other patients and therefore were inconsistent with the high trough concentrations measured. The most plausible explanation is therefore that the previous dose was ingested less than 24 h before the predose sample was collected, but since few of these values were obtained and the values were relatively low compared to the peak concentrations, they did not significantly impact model parameter values and were included in the analysis. Similarly, we tested the alternative approach of excluding all concentrations BLQ altogether, and the model parameters did not significantly change.

The model adequately fit the data, as shown in the visual predictive checks (VPCs) in Fig. 2, which highlight the differences in the concentration-time profiles between

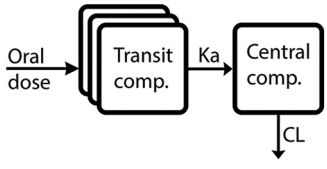


**FIG 1** Graphical overview of the structural pharmacokinetic model. comp., compartment.

**TABLE 2** Pediatric pharmacokinetic parameter estimates for ethionamide[c]

| Parameter | Estimate of typical value (95% CI) | Estimate of % variability[b] (95% CI), variability type |
|---|---|---|
| CL[a] (liters/h) without rifampin | 8.88 (8.21, 9.71) | 17.0 (13.9, 20.7), IIV |
| Rifampin effect on CL (%) | +16.0 (+6.3, +27.0) | |
| *V* (liters)[a] | 21.4 (20.2, 22.8) | |
| Bioavailability for HIV-uninfected patients | 1 (fixed) | 24.9 (21.2, 29.5), IOV |
| Effect of HIV on bioavailability (%) | −22.3 (−30.6, −13.4) | |
| MTT with oral administration (h) | 1.07 (0.982, 1.178) | 97.0 (83.7, 111), IOV |
| Effect of NGT on MTT (%) | −67.9 (−76.0, −59.5) | |
| No. of transit compartments | 2.31 (1.84, 2.83) | |
| $k_a$ ($h^{-1}$) | 0.867 (0.774, 0.957) | 36.3 (27.1, 46.6), IOV |
| Maturation of CL | | |
| $PMA_{50,CL}$ (yr) | 0.876 (0.713, 1.03) | |
| $\gamma_{mat,CL}$ | 2.60 (1.43, 4.75) | |
| Maturation of absorption | | |
| $Scale_{Abs}$ (fold) | 2.43 (2.38, 2.50) | |
| $\gamma_{mat,Abs}$ (1/yr) | 1 (fixed) | |
| Proportional error (%) | 17.2 (15.7, 18.8) | |
| Additive error ($\mu$g/ml) | 0.0138 (0.0123, 0.0153) | |

[a]Clearance depends on age and weight due to maturation and allometric scaling. Volume of distribution depends on weight due to allometric scaling. These values refer to those for a typical 13-kg child with completed maturation.
[b]Variability is reported here as an approximate coefficient of variation (in percent).
[c]CI, confidence interval, obtained by sampling importance-resampling (SIR); IIV, interindividual variability; IOV, interoccasion variability; CL, clearance; *V*, volume of distribution; $PMA_{50,CL}$ postmenstrual age at which maturation of clearance is 50% complete; $\gamma_{mat,CL}$, shape factor for maturation of clearance; $k_a$, absorption rate constant; MTT, mean transit time for absorption; NGT, nasogastric tube; $Scale_{Abs}$, scaling factor for maturation of absorption; $\gamma_{mat,Abs}$, shape factor for maturation of absorption.

administration via an NGT versus administration via the oral route, age below 1 year versus age above 1 year, and HIV infection status. VPCs with alternative stratifications are shown in Fig. S2 to S4. Conditional weighted residuals (Fig. S5) indicated underprediction of the predose concentrations. However, most of these values were BLQ, so this trend does not indicate model misspecification but is an artifact of the imputation to LLOQ/2.

**Dosing optimization.** Model-based predictions of weight-banded pediatric exposures are compared to predicted adult exposures in Fig. 3. The adult reference values of the area under the concentration-time curve (AUC) from 0 to 24 h ($AUC_{0-24}$) and maximum concentration ($C_{max}$) were 27.3 $\mu$g·h/ml and 3.94 $\mu$g/ml, respectively, as predicted by our model for adults in the 50- to 70-kg weight band receiving a 750-mg dose. The currently recommended dose of 20 mg/kg, as well as the recent weight-banded WHO recommendations, generally achieves a higher AUC and a higher $C_{max}$ than the target exposure in adults. This is especially true for children whose weight is <6 kg, who display the highest predicted concentrations due to their rapid absorption and their incomplete maturation of clearance.

The proposed optimized doses detailed in Table 3 achieve exposures more in line with adult values in most weight bands, as shown in Fig. 3.

## DISCUSSION

We developed a population pharmacokinetic model that describes ethionamide concentrations in children well, characterizing the effects of body weight and age.

Simulations from our model show that constant milligram-per-kilogram dosing achieves uneven exposures, with children who weigh <6 kg and (to a minor extent) those who weigh >20 kg attaining higher exposures than 50- to 70-kg adults receiving ethionamide at 750 mg. The recent WHO weight-banded dosing regimen (11), while representing an improvement in terms of facilitating dosing with the current formulations, is restricted to children who weigh >5 kg and does not adequately account for maturation in infants, who are therefore predicted to achieve comparatively higher concentrations. The alternative dosing that we suggest harmonizes the exposure across all weight bands, in particular, reducing the concentrations in very small children

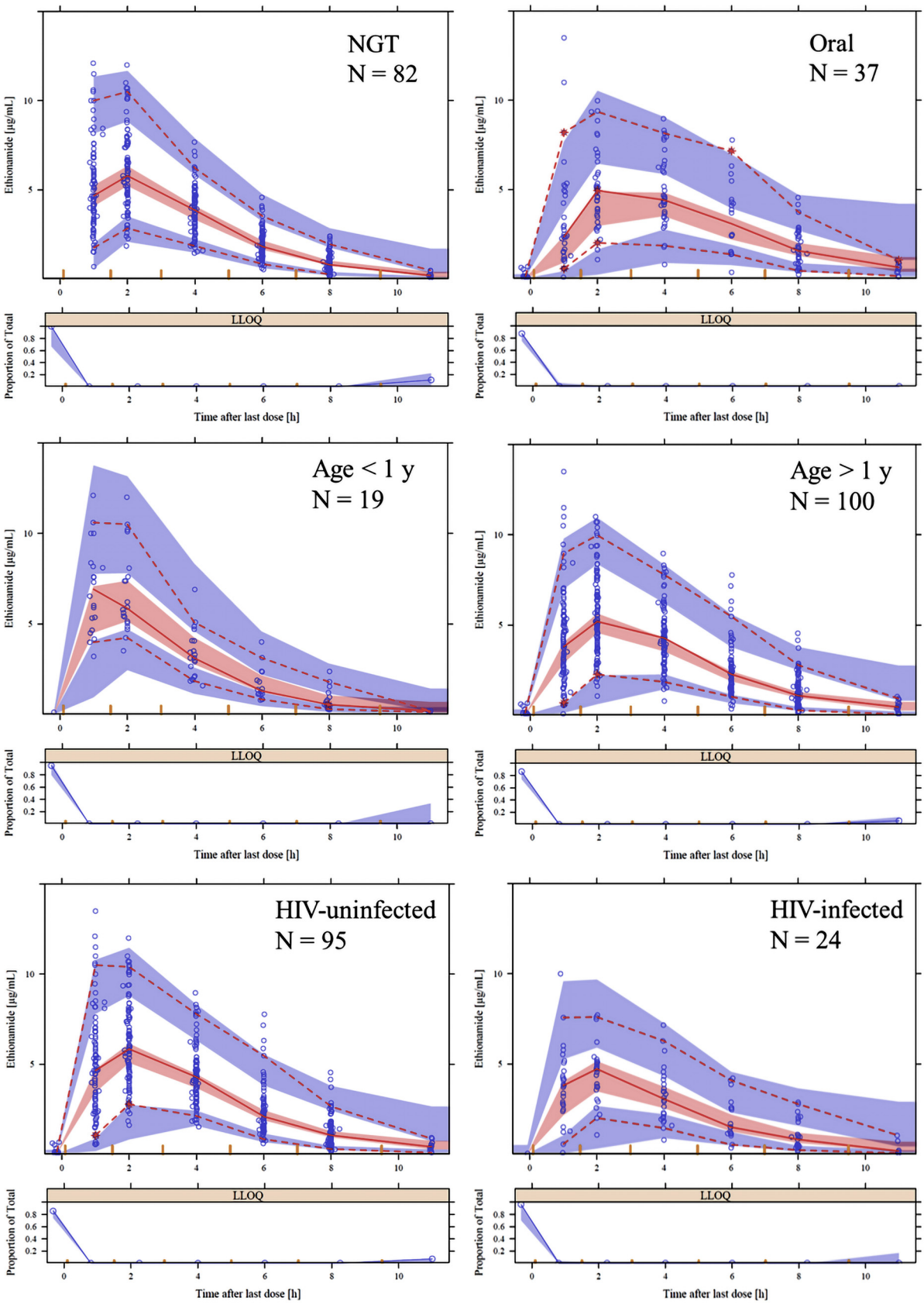


**FIG 2** Visual predictive check (VPC) of ethionamide concentration versus time after the last dose, stratified on administration method (i.e., nasogastric tube or oral) (top), age under 1 year or over 1 year (middle), and HIV infection status (bottom). The solid lines represent the 50th

(Continued on next page)

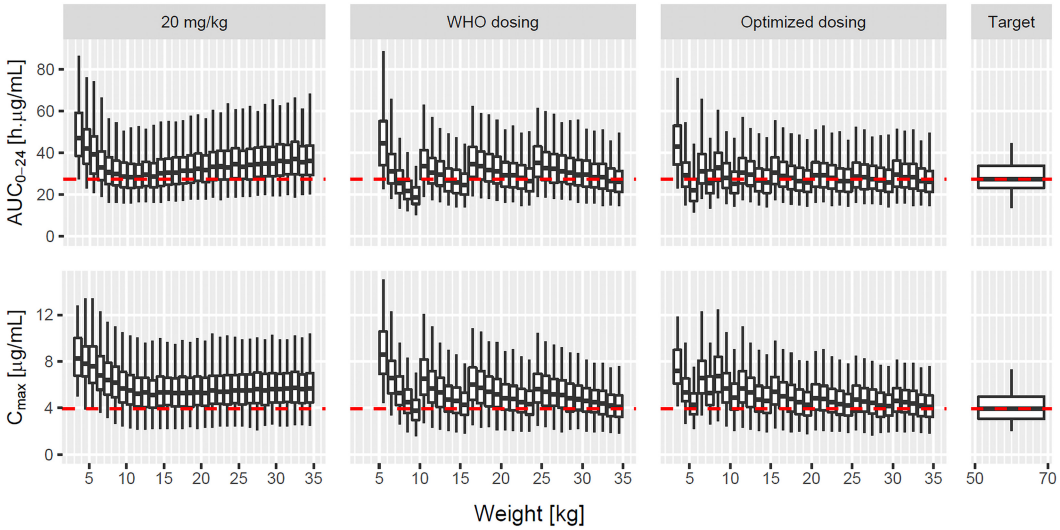


**FIG 3** Simulated ethionamide $AUC_{0-24}$ (top) and $C_{max}$ (bottom) versus body weight for the 20-mg/kg dose (left), weight-banded WHO dose recommendations (second from left), and suggested optimized weight-banded doses (third from left), as well as target model predictions in 50- to 70-kg adults receiving 750 mg (right). Note that WHO dose recommendations start at 5 kg. Dashed lines are predictions of the median values for adults used as dose optimization targets ($AUC_{0-24}$, 27.34 $\mu$g·h/ml; $C_{max}$, 3.94 $\mu$g/ml) in 50- to 70-kg adults receiving 750 mg. All simulations were performed assuming no HIV infection, no rifampin cotreatment, and oral dosing of ethionamide without NGT.

(weight, <6 kg), in whom the current constant milligram-per-kilogram approach produces median values of $C_{max}$ nearly twice as high as the predicted exposure in adults after a 750-mg dose. Although $C_{max}$ values are more controlled under our suggested dosing, they are still high compared to the adult target, and it may be warranted to consider twice-daily dosing in these small children, at least in cases where adverse effects are observed.

Our analysis found lower ethionamide bioavailability in HIV-infected patients. This confirms the findings of an earlier study (14), but the underlying reason for the effect is unclear. We tested whether the effect was related to a drug-drug interaction with a particular ART regimen, but no significant difference was found between the three groups receiving treatment for HIV infection (the ART-naive group and the groups receiving lopinavir-ritonavir- and efavirenz-based ART). If the effect is not a drug-drug interaction but, indeed, is related to HIV *per se*, a possible explanation may be found in the inflammation of the intestinal mucosa caused by HIV infection (15), which may affect drug absorption (16).

Rifampin cotreatment was found to increase ethionamide clearance by 16%. Several ethionamide elimination pathways could be affected by rifampin, including the most prominent metabolic pathway, flavin-containing monooxygenases (FMOs) (17). FMOs are also responsible for the activation of ethionamide (18), so it is unclear whether this interaction may affect or not affect ethionamide efficacy. One earlier study explored the effect of rifampin cotreatment on ethionamide concentrations and did not find a significant difference in half-life ($P = 0.10$), elimination rate constant ($P = 0.11$), or clearance ($P = 0.37$) (14). The effect that we detected was modest in size, and the previous study may not have been powered to detect it. Moreover, the use of population pharmacokinetic modeling and the greater number of patients in our analysis are expected to lead to a higher statistical power.

**FIG 2** Legend (Continued)
percentiles of the observed data and the dashed lines represent the 5th and 95th percentiles of the observed data. The shaded areas represent the model-predicted 95% confidence intervals for the same percentiles. The dots are the observed concentrations. The smaller panels under each VPC are VPCs of the proportion of observations below the lower limit of quantification (LLOQ). The solid line shows the proportion of LLOQ observations in the data, and the shaded area is the 95% confidence interval of the proportions of model-predicted LLOQ observations.

**TABLE 3** Suggested optimized doses for different weight bands in a pediatric population[a]

| wt band (kg) | No. of tablets | | Daily dose (mg) |
|---|---|---|---|
| | 250 mg | 125 mg | |
| 3 to <6 | 0.25 | 0.5 | 62.5 |
| 6 to <8 | 0.5 | 1 | 125 |
| 8 to <11 | 0.75 | 1.5 | 187.5 |
| 11 to <15 | 1 | 2 | 250 |
| 15 to <20 | 1.25 | 2.5 | 312.5 |
| 20 to <25 | 1.5 | 3 | 375 |
| 25 to <30 | 1.75 | 3.5 | 437.5 |
| 30 to <35 | 2 | 4 | 500 |

[a]Doses are given as multiples of 62.5 mg, equivalent to a 250-mg tablet split in quarters or a 125-mg tablet split in half.

An effect of isoniazid cotreatment on ethionamide bioavailability and clearance has recently been reported (19). The same trend of higher ethionamide exposure with isoniazid cotreatment was observed in this analysis as well, but since only 7 children in this study were on isoniazid-free regimens, this effect could not be robustly characterized, and it was therefore not included in the final model.

Maturation of clearance significantly improved the model fit, even though limited data for very young children were available.

Maturation of absorption improved the predictions but did not completely explain the rapid absorption in very young children, as shown in Fig. 1. The data suggest an absorption for children under 1 year old even faster than what was captured in the model. Maturation of the volume of distribution, possibly due to changes in body composition, was examined as an alternative explanation, but it did not improve the model fit. Absorption may be different in these very young children because of differences in the gastrointestinal tract in early infancy, but we lack the information to explain the phenomenon. The effect may be partly explained by a biexponential concentration-time profile being more prominent in young children. Such a profile has been observed for intravenous dosing of ethionamide in adults, with an initial distribution phase occurring during the first 40 min after dosing (20). A two-compartment disposition model was tested but did not significantly improve the fit, possibly because our sampling schedule (with the first observation being at 1 h postdose) was not suitable to capture this effect.

Comparing exposures to historical values and defining a clear range for adult exposure proved difficult, as published values varied greatly between and within studies. In Table 4 we present a comparison of the findings of different published pharmacokinetic analyses of ethionamide. For each study, we present the published AUC, the dose, and the population in which it was measured, as well as AUC scaled to dose and allometry, for side-by-side comparisons of AUCs across studies. The values from our study were generally closer to the values reported for healthy volunteers than those reported for adult patients. Our findings also differ from those of a study published by Thee et al. (14) with a cohort of 31 children from the Cape Town, South Africa, region very similar to the cohort evaluated in our study. Large interindividual differences were also observed within each study; in spite of using similar dose amounts, Grönroos and Toivanen (21), Zhu et al. (22), and Auclair et al. (23) all reported wide ranges of AUCs (up to 14-fold) in adults within each study. While the AUCs in our pediatric population also displayed high variability, we were able to attribute most of the variability either to covariates or to specific sources, such as large interoccasion variability in drug absorption. The high variability in historical AUC values between and within studies made it difficult to choose a single target exposure, leading us to prefer a value predicted by our own model.

The study has some limitations. Only a small number of infants were included in the analysis, and in those few infants, the overlapping and confounding effects of age, weight, food administration with the dose, and administration procedure (oral admin-

**TABLE 4** Comparison of populations and AUCs between this and previous studies of ethionamide[i]

| Study or authors (reference) | Yr | Location | TB status | Median (range) age (yr) | Median (range) wt (kg) | Median (range) dose | Formulation | *N* | Median (range) published AUC[a] (μg·h/ml) | Predicted[b] AUC (μg·h/ml) after 750-mg dose in a typical 60-kg adult |
|---|---|---|---|---|---|---|---|---|---|---|
| This study | 2019 | South Africa | TB, MDR-TB | 2.6 (0.23–15) | 12.5 (2.5–66) | 20 (10–25) mg/kg | | 119 | 28.1 (9.45–57.7) | 26.8 |
| Grönroos and Toivanen (21) | 1964 | Finland | TB | 52 (34–63) | 65 (56–101) | 500 mg | Uncoated tablet | 19 | 4.6 (1.4–17.2) ($AUC_{0-9}$) | 7.4 ($AUC_{0-9}$) |
| Mattila et al. (47) | 1968 | Finland | TB | NA | 60 (imputed) | 500 mg | Film-coated tablet | 15 | 15.6[c] ($AUC_{0-6}$) | 23.3 ($AUC_{0-6}$) |
| Tiitinen (48) | 1969 | Finland | TB | NA | 60 (imputed) | 500 mg | | 20 | 10.0[c] (4.2–15.6) ($AUC_{0-5}$) | 15.0 ($AUC_{0-5}$) |
| Jenner and Ellard (49) | 1981 | UK | Healthy | 44 | 65 | 500 mg | | 1 | 15.67[c] | 25.3 |
| Jenner et al. (50) | 1984 | Malaysia | Healthy | NA | 60 (imputed) (51) | 250 mg | | 9 | 8.99[c] | 27.0 |
| Jenner and Smith (20) | 1987 | UK | Healthy | NA | 65 (imputed) (49) | 500, 25 mg | i.v. | 1 | 20.25 (0.92, i.v.) | 32.3 (29.3, i.v.) |
| Peloquin et al. (52) | 1991 | USA | Healthy | 32 (19–52)[g] | 80 (64–99)[g] | 500 mg | Oral | 12 | 10.34 (2.29)[h] | 19.2 |
| Auclair et al. (23) | 2001 | USA | Healthy | 36 (24–47) | 77 (61–96) | 500 mg | | 12 | 10.0 (2.7–19) | 18.1 |
| Zhu et al. (22)[d] | 2002 | USA | TB | 45 (6.7–79) | 60 (25–92) | 500 (250–1,000) mg | | 55 | 3.95 (1.47–21.2) | 5.9 |
| Thee et al. (14) | 2011 | South Africa | TB, TB-M, MDR-TB | 2.8 (0.3–12) | 12 (4.9–35) | 17.9 (15–20) mg/kg | | 31 | 12.5[e] (6.57) | 13.1 or 15.7[f] |
| Korth-Bradley et al. (53) | 2014 | USA | Healthy | 28 (18–53)[g] | 74 (55–94)[g] | 250 mg | Film-coated talets | 40 | 7.67 (1.69)[h] | 26.9 |
| Hemanth Kumar et al. (54) | 2018 | India | MDR-TB | 16 (5–18) | 33 (15–58) | 15.3 (11.4–25.0) mg/kg | | 25 | 14.78 (5.2–24.0) ($AUC_{0-8}$) | 14.3 ($AUC_{0-8}$) |

[a]If not specified, the values are $AUC_{0-24}$ at steady state or $AUC_{0-\infty}$ after a single dose, as applicable. If extrapolation or calculation of $AUC_{0-\infty}$ was not possible, $AUC_{0-t}$ was used and is specifically stated in parentheses. We are aware that using allometric scaling to adjust $AUC_{0-t}$ introduces some bias, but the values are still included to ease comparison.

[b]Model-predicted AUC for a typical HIV-uninfected adult with TB in the middle of the most common weight band (50 to 70 kg).

[c]Median of individual AUCs or the AUC from mean/median concentrations calculated by the linear trapezoidal method with data obtained from digitized concentration-time graphs or tables.

[d]Healthy volunteers (group C, $n = 12$) were excluded, as they were the same cohort evaluated in the study of Auclair et al. (23). Doses are total daily doses.

[e]The mean and standard deviation AUC were calculated by pooling means and variances for all reported groups and both occasions.

[f]$AUC_{0-\infty}$ = 15.7 μg·h/ml when further adjusted for HIV and rifampin effects, according to our model (77.7% bioavailability for 12/31 HIV-infected patients, 116% clearance for 15/31 patients receiving rifampin).

[g]The values represent the mean (range).

[h]The values represent the mean (standard deviation).

[i]TB, tuberculosis; TB-M, tuberculosis meningitis; MDR-TB, multidrug-resistant tuberculosis; *N*, number of subjects; AUC, area under the concentration-time curve; NA, not available; i.v., intravenous administration.

istration of a whole tablet versus a crushed tablet or administration via a nasogastric tube) limited what the model could identify. The lack of accurate information on gestational age at birth added to this complexity, as children born preterm may be less mature than their postnatal age would explain. The lack of early samples after dosing (<1 h) also limited our capability to characterize absorption. We used an empirical mathematical model for the maturation of absorption, and this enabled us to describe the effect, although the physiological changes underpinning it are unclear. Another area that warrants further investigation is the effect of HIV coinfection. Several studies in the literature report either lower or higher concentrations of antitubercular drugs in HIV-infected patients, and as recently summarized by Daskapan et al., the results are discordant even for the same drug (24). Decreases in concentration have recently been reported in HIV-coinfected children for other anti-TB drugs (9, 25). Studying this effect and its impact on dosing would be important. The recommendations assume that the children are HIV uninfected.

Another limitation is that no established pharmacodynamic or clinical target was available to guide the dosing. Our study did not assess efficacy, but it is reasonable to assume that the exposure-response relationships between children and adults are similar (26). However, patient progress should be monitored under this new dosing.

In suggesting new doses, we have assumed that pediatric formulations are bioequivalent to the adult formulations used in this study. While this is generally a reasonable assumption, several studies with other anti-TB drugs have identified bioequivalence issues between certified pediatric and adult formulations (27–29).

In conclusion, we propose a model that accurately describes the effect of weight and age on the pharmacokinetics of ethionamide in children. Cotreatment with rifampin moderately increased ethionamide clearance. Crushing of the tablets for oral administration or the use of a nasogastric tube affected the speed but not the extent of ethionamide absorption. We also observed that HIV-infected patients had lower bioavailability, but with the limited current data, we were unable to confirm the precise cause of this effect.

Based on the predicted exposures according to the developed model, we have suggested a new dosing strategy for ethionamide in children, which is expected to improve tolerability and reduce adverse effects.

## MATERIALS AND METHODS

**Clinical studies.** Data on the pharmacokinetics of ethionamide in children were pooled from 2 observational clinical studies conducted in Cape Town, South Africa: MDR-PK1 (9) (2011 to 2015) and DATiC (30, 31) (2012 to 2017).

In MDR-PK1, children were included if they were under 15 years old and routinely treated for probable or confirmed MDR-TB (and with antiretroviral drugs if they were HIV infected). They were treated with multidrug regimens consistent with local and international guidance at the time: at least four effective drugs, including ethionamide plus a fluoroquinolone, an injectable drug, and combinations of other drugs (terizidone, high-dose isoniazid, pyrazinamide, and ethambutol) for 12 to 18 months.

In DATiC, young HIV-infected or -uninfected children were treated for drug-susceptible TB with combination therapy, including isoniazid, rifampin, and pyrazinamide. If a fourth drug was indicated, ethionamide was given to children if it was preferred over ethambutol by the attending clinician.

Informed consent was provided by the parent(s) or legal guardian of all participants, and assent was provided by all participants aged 7 years or older. Ethics approval was provided by the Health Research Ethics Committees of Stellenbosch University and the University of Cape Town.

In both studies, the children received once-daily ethionamide doses of approximately 20 mg/kg (250-mg Sanofi-Aventis tablets) for at least 2 weeks prior to sampling. On the day of pharmacokinetic sampling, the dose in MDR-PK1 was adjusted to exactly 20 mg/kg, and smaller children received crushed tablets due to the lack of child-friendly formulations, and a nasogastric tube (NGT) was often used. Ethionamide was coadministered with other first- or second-line antituberculosis medications. Antiretroviral therapy (ART), if given, was administered 1 h after (MDR-PK1) or together with (DATiC) antituberculosis medications.

The dose was administered by the study team after an overnight fast, and blood samples were collected at 0 (predose), 1, 2, 4, 8, and either 6 or 11 h postdose in MDR-PK1 and at 0, 1, 2, 4, 6, and 8 h postdose in DATiC. Food was offered 1 h after the dose.

Ethionamide plasma concentrations were determined from 20 $\mu$l of plasma using a validated liquid chromatography-tandem mass spectrometry (LC-MS/MS) assay method developed in the Division of Clinical Pharmacology, University of Cape Town. The samples were processed with a protein precipitation extraction method using acetonitrile, followed by high-performance liquid chromatography with MS/MS

detection. Neostigmine was used as the internal standard. The extraction procedure was followed by liquid chromatographic separation using a Discovery HS F5 analytical column (5 cm by 2.1 mm; particle size, 3 $\mu$m; Supelco). An AB Sciex API4000 mass spectrometer at unit resolution in the multiple-reaction-monitoring (MRM) mode was used to monitor the transition of the protonated precursor ions at *m/z* 167.1 to the product ions at *m/z* 106.1 and the protonated molecular ions at *m/z* 224.2 to the product ions at *m/z* 72.1 for the internal standard. Electrospray ionization (ESI) was used for ion production. Accuracy and precision were assessed over three consecutive, independent runs, with inter- and intraday coefficients of variation being below 7% for all quality control samples. The assay was validated over the concentration range of 0.0313 $\mu$g/ml (i.e., the lower limit of quantification [LLOQ]) to 16.0 $\mu$g/ml, with the calibration curve fitting a quadratic regression (weighted by 1/concentration).

**Population pharmacokinetic model.** The data were analyzed with nonlinear mixed-effects modeling in NONMEM (version 7.4) software (32). Parameter estimates were obtained by first-order conditional estimation with interaction (FOCEI) and saddle reset (33) to overcome issues with stability and practical identifiability.

Model building was performed stepwise, with all parameters being reestimated at every step, and was guided by drops in the NONMEM objective function value (OFV). Nested models with 1 additional degree of freedom were considered significantly improved at a *P* value of $<0.05$ if the OFV decreased by 3.84 (34). The models were further evaluated using goodness-of-fit plots and visual predictive checks (VPCs) (35, 36), generated using R software (37) and the Perl-Speaks-NONMEM (PsN), Xpose4, and Pirana programs (38). Each model change was also evaluated in relation to *a priori* hypotheses and the physiological plausibility of the results.

The structural model was selected from candidates, including models with a one- or a two-compartment distribution with first-order elimination and first-order absorption with or without a lag time or transit compartments. Interindividual variability (IIV) and interoccasion variability (IOV) were assumed to follow lognormal distributions. The statistical model was selected from combinations of IOV on absorption parameters and IIV on clearance or the volume of distribution, based on statistical significance, physiological plausibility, and model robustness. Models with IIV and IOV on the same parameter were excluded as practically nonidentifiable due to the lack of observed repeated occasions. Observations below the LLOQ (BLQ) were imputed to LLOQ/2, except for consecutive values in a series, which were excluded from the fit (the M6 method) (39), but were included in VPCs. Residual variability was assumed to have an additive and a proportional element, with the additive error being bound to be at least 20% of the LLOQ to minimize the effect of the BLQ imputation.

The effect of body size was described using allometric scaling of clearance (CL) and the volume of distribution (*V*), using the recommended exponent values of 0.75 and 1, respectively (13, 40). Besides total body weight, fat-free mass (41) was explored as an alternative size descriptor.

Maturation of clearance was explored according to equation 3 (13, 40):

$$\text{maturation} = \frac{\text{PMA}^{\gamma_{\text{mat}}}}{\text{PMA}_{50}^{\gamma_{\text{mat}}} + \text{PMA}^{\gamma_{\text{mat}}}} \quad (3)$$

where PMA is postmenstrual age, $\text{PMA}_{50}$ is the PMA at which maturation is 50% complete, and $\gamma_{\text{mat}}$ is the shape factor. No information on gestational age at birth was available, so PMA was assumed to be the postnatal age plus 9 months.

After the inclusion of allometric scaling and maturation, further covariate relations were systematically explored using a stepwise covariate modeling (38) ($P_{\text{forward}} = 0.05$, $P_{\text{backward}} = 0.01$). Relations indicated to be significant by this procedure were included only if the effect was deemed physiologically plausible and improvements in stratified VPCs and goodness-of-fit metrics were observed. The effects of the following covariates were explored on all parameters: HIV infection status, ethnicity (black versus mixed race), sex, age, concomitant use of each antituberculosis and antiretroviral drug, study, and WHO Z-scores (Z-scores for weight for age, height for age, and body mass index for weight) (42, 43). The effect of the administration procedure (oral whole tablet, oral crushed tablet, or crushed tablet through an NGT) was tested on the absorption parameters only. All continuous covariates were tested with linear or broken-stick models, except for the effect of age, for which exponential and sigmoidal functions were also investigated. The final model was tested by removing each of the included relationships to ascertain their impact and statistical significance in the final model.

The precision of the final parameter estimates was determined using the sampling importance-resampling procedure (44) implemented in PsN with the default settings.

**Dosing optimization.** Since no established pharmacokinetic target is available in children, the aim of our dose optimization exercise was to match the adult exposure (26, 45). We selected as the target adult exposure the median value of the area under the concentration-time curve (AUC) profile predicted by our model extrapolated to adults in the 50- to 70-kg weight band receiving the currently recommended dose of 750 mg. Monte Carlo simulations of pediatric exposures from the final model were compared to the target value, and dose adjustments were suggested where necessary. Previously published reports on ethionamide pharmacokinetics were identified and summarized. $\text{AUC}_{0-24}$ or the AUC from time zero to infinity ($\text{AUC}_{0-\infty}$) was extracted, if available; otherwise, the AUC from 0 h to time *t* ($\text{AUC}_{0-t}$) was used. If AUC was not specified in the original publications, it was calculated by the linear trapezoidal method from published time-concentration tables or digitized plots. To facilitate the comparison of AUC values between studies, the AUC values were standardized to a patient weighing 60 kg (the middle of the 50- to 70-kg weight band) using allometric scaling and to a dose of 750 mg, assuming linear kinetics (i.e., $\text{AUC}_{0-\infty}$ = dose/clearance).

The exposures in each pediatric weight band were simulated using an *in silico* population ($n = 43,400$) with combinations of weight and age previously reported in TB-infected children by Svensson et al. (46).

Pediatric exposure simulations were generated for 20-mg/kg dosing and for the WHO weight-banded guidelines (11). Doses were then optimized to match the target adult exposure using weight banding and currently available tablet sizes. We used weight bands from a recent dosing optimization of levofloxacin (9) and assumed that the smallest feasible dose was 62.5 mg (equivalent to a quarter of a 250-mg tablet or half of a 125-mg tablet). We selected the dose with the median predicted AUC closest to the adult target in each weight band. While AUC was used as the dose optimization target, the simulated values of the maximum concentration ($C_{max}$) were also monitored.

## SUPPLEMENTAL MATERIAL

Supplemental material is available online only.

**SUPPLEMENTAL FILE 1**, PDF file, 1.4 MB.

## ACKNOWLEDGMENTS

We thank Eva Germovšek and Erik Melander from Uppsala University for valuable discussions on scaling, maturation, and how to compare drug exposures between studies.

This work was supported by the Swedish Foundation for International Cooperation in Research and Higher Education (STINT) jointly with the South African National Research Council, National Research Foundation (NRF; grant number: 101575). The MDR-PK1 study was supported by The Eunice Kennedy Shriver National Institute of Child Health and Human Development (NICHD) of the National Institutes of Health under award number R01HD069169 (to A.C.H.). The DATiC study was supported by the Eunice Kennedy Shriver National Institute of Child Health and Human Development (NICHD) of the National Institutes of Health under award number R01HD069175 to H.M. H.M. is funded by the Wellcome Trust (grant 206379/Z/17/Z), and A.C.H. is funded by the South African National Research Foundation under a SARCHI Chair. H.J.Z. is funded by the South African Medical Research Council.

## REFERENCES

1. Jenkins HE, Tolman AW, Yuen CM, Parr JB, Keshavjee S, Perez-Velez CM, Pagano M, Becerra MC, Cohen T. 2014. Incidence of multidrug-resistant tuberculosis disease in children: systematic review, and global estimates. Lancet 383:1572–1579. https://doi.org/10.1016/S0140-6736(14)60195-1.
2. Thee S, Garcia-Prats AJ, Donald PR, Hesseling AC, Schaaf HS. 2016. A review of the use of ethionamide and prothionamide in childhood tuberculosis. Tuberculosis (Edinb) 97:126–136. https://doi.org/10.1016/j.tube.2015.09.007.
3. World Health Organization. 2016. WHO guidelines for the programmatic management of drug resistant tuberculosis: 2016 update. World Health Organization, Geneva, Switzerland.
4. Donald PR, Seifart HI. 1989. Cerebrospinal fluid concentrations of ethionamide in children with tuberculous meningitis. J Pediatr 115:483–486. https://doi.org/10.1016/s0022-3476(89)80862-5.
5. Hughes IE, Smith H. 1962. Ethionamide: its passage into the cerebrospinal fluid in man. Lancet i:616–617. https://doi.org/10.1016/s0140-6736(62)91602-1.
6. Bennett JE, Dolin R, Blaser MJ, Mandell GL, Douglas RG. 2014. Mandell, Douglas, and Bennett's principles and practice of infectious diseases. Elsevier Health Sciences, Philadelphia, PA.
7. Chan ED, Laurel V, Strand MJ, Chan JF, Huynh M-L, Goble M, Iseman MD. 2004. Treatment and outcome analysis of 205 patients with multidrug-resistant tuberculosis. Am J Respir Crit Care Med 169:1103–1109. https://doi.org/10.1164/rccm.200308-1159OC.
8. Nathanson E, Gupta R, Huamani P, Leimane V, Pasechnikov AD, Tupasi TE, Vink K, Jaramillo E, Espinal MA. 2004. Adverse events in the treatment of multidrug-resistant tuberculosis: results from the DOTS-Plus initiative. Int J Tuberc Lung Dis 8:1382–1384.
9. Denti P, Garcia-Prats AJ, Draper HR, Wiesner L, Winckler J, Thee S, Dooley KE, Savic RM, McIlleron HM, Schaaf HS, Hesseling AC, Denti P, Garcia-Prats AJ, Draper HR, Wiesner L, Winckler J, Thee S, Dooley KE, Savic RM, McIlleron HM, Schaaf HS, Hesseling AC. 2018. Levofloxacin population pharmacokinetics in South African children treated for multidrug-resistant tuberculosis. Antimicrob Agents Chemother 62:e01521-17. https://doi.org/10.1128/AAC.01521-17.
10. South Africa National Department of Health. 2017. Standard treatment guidelines and essential medicines list for South Africa—hospital level paediatrics. South Africa National Department of Health, Pretoria, South Africa.
11. World Health Organization. 2019. WHO consolidated guidelines on drug-resistant tuberculosis treatment. World Health Organization, Geneva, Switzerland.
12. Savic RM, Jonker DM, Kerbusch T, Karlsson MO. 2007. Implementation of a transit compartment model for describing drug absorption in pharmacokinetic studies. J Pharmacokinet Pharmacodyn 34:711–726. https://doi.org/10.1007/s10928-007-9066-0.
13. Anderson BJ, Holford N. 2008. Mechanism-based concepts of size and maturity in pharmacokinetics. Annu Rev Pharmacol Toxicol 48:303–332. https://doi.org/10.1146/annurev.pharmtox.48.113006.094708.
14. Thee S, Seifart HI, Rosenkranz B, Hesseling AC, Magdorf K, Donald PR, Schaaf HS. 2011. Pharmacokinetics of ethionamide in children. Antimicrob Agents Chemother 55:4594–4600. https://doi.org/10.1128/AAC.00379-11.
15. Brenchley JM, Douek DC. 2008. HIV infection and the gastrointestinal immune system. Mucosal Immunol 1:23–30. https://doi.org/10.1038/mi.2007.1.
16. Peuhkuri K, Vapaatalo H, Korpela R. 2010. Even low-grade inflammation impacts on small intestinal function. World J Gastroenterol 16:1057–1062. https://doi.org/10.3748/wjg.v16.i9.1057.
17. Niemi M, Backman JT, Fromm MF, Neuvonen PJ, Kivisto KT. 2003. Pharmacokinetic interactions with rifampicin: clinical relevance. Clin Pharmacokinet 42:819–850. https://doi.org/10.2165/00003088-200342090-00003.
18. Wang F, Langley R, Gulten G, Dover LG, Besra GS, Jacobs WR, Jr, Sacchettini JC. 2007. Mechanism of thioamide drug action against tu-

berculosis and leprosy. J Exp Med 204:73–78. https://doi.org/10.1084/jem.20062100.
19. Chirehwa M, Court R, De Kock M, Wiesner L, de Vries N, Harding J, Gumbo T, Denti P, Maartens G, McIlleron H. 2019. Ethionamide population pharmacokinetics/pharmacodynamics during treatment of multidrug-resistant tuberculosis, p S303. Abstr 50th World Conference Lung Health Int Union Tuberc Lung Dis, Hyderabad, India.
20. Jenner PJ, Smith SE. 1987. Plasma levels of ethionamide and prothionamide in a volunteer following intravenous and oral dosages. Lepr Rev 58:31–37. https://doi.org/10.5935/0305-7518.19870004.
21. Grönroos JA, Toivanen A. 1964. Blood ethionamide levels after administration of enteric-coated and uncoated tablets. Curr Ther Res Clin Exp 6:105–114.
22. Zhu M, Namdar R, Stambaugh JJ, Starke JR, Bulpitt AE, Berning SE, Peloquin CA. 2002. Population pharmacokinetics of ethionamide in patients with tuberculosis. Tuberculosis (Edinb) 82:91–96. https://doi.org/10.1054/tube.2002.0330.
23. Auclair B, Nix DE, Adam RD, James GT, Peloquin CA. 2001. Pharmacokinetics of ethionamide administered under fasting conditions or with orange juice, food, or antacids. Antimicrob Agents Chemother 45:810–814. https://doi.org/10.1128/AAC.45.3.810-814.2001.
24. Daskapan A, Idrus LR, Postma MJ, Wilffert B, Kosterink JGW, Stienstra Y, Touw DJ, Andersen AB, Bekker A, Denti P, Hemanth Kumar AK, Jeremiah K, Kwara A, McIlleron H, Meintjes G, van Oosterhout JJ, Ramachandran G, Rockwood N, Wilkinson RJ, van der Werf TS, Alffenaar J-W. 2019. A systematic review on the effect of HIV infection on the pharmacokinetics of first-line tuberculosis drugs. Clin Pharmacokinet 58:747–766. https://doi.org/10.1007/s40262-018-0716-8.
25. Guiastrennec B, Ramachandran G, Karlsson MO, Kumar AKH, Bhavani PK, Gangadevi NP, Swaminathan S, Gupta A, Dooley KE, Savic RM. 2018. Suboptimal antituberculosis drug concentrations and outcomes in small and HIV-coinfected children in India: recommendations for dose modifications. Clin Pharmacol Ther 104:733–741. https://doi.org/10.1002/cpt.987.
26. Food and Drug Administration. 2014. General clinical pharmacology considerations for pediatric studies for drugs and biological products. Guidance for industry. Food and Drug Administration, Silver Spring, MD.
27. McIlleron H, Wash P, Burger A, Folb P, Smith P. 2002. Widespread distribution of a single drug rifampicin formulation of inferior bioavailability in South Africa. Int J Tuberc Lung Dis 6:356–361.
28. McIlleron H, Hundt H, Smythe W, Bekker A, Winckler J, van der Laan L, Smith P, Zar HJ, Hesseling AC, Maartens G, Wiesner L, van Rie A. 2016. Bioavailability of two licensed paediatric rifampicin suspensions: implications for quality control programmes. Int J Tuberc Lung Dis 20:915–919. https://doi.org/10.5588/ijtld.15.0833.
29. Garcia-Prats AJ, Purchase SE, Osman M, Draper HR, Schaaf HS, Wiesner L, Denti P, Hesseling AC, Garcia-Prats AJ, Purchase SE, Osman M, Draper HR, Schaaf HS, Wiesner L, Denti P, Hesseling AC. 2019. Pharmacokinetics, Safety, and dosing of novel pediatric levofloxacin dispersible tablets in children with multidrug-resistant tuberculosis exposure. Antimicrob Agents Chemother 63:e01865-18. https://doi.org/10.1128/AAC.01865-18.
30. Denti P, Gonzalez-Martinez C, Winckler J, Bekker A, Zar H, Davies G, van Rie A, McIlleron HM. 2017. Pharmacokinetics of rifampicin in African children: evaluation of the new WHO dosing guidelines, p S203. Abstr 48th Union World Conf Lung Health, Guadalajara, Mexico.
31. National Library of Medicine. 2019. Optimal dosing of 1st line antituberculosis and antiretroviral drugs in children (a pharmacokinetic study) (DATiC). National Library of Medicine, Bethesda, MD. https://clinicaltrials.gov/ct2/show/NCT01637558.
32. Beal S, Sheiner LB, Boeckmann A, Bauer RJ. 2017. NONMEM 7.4 user's guides. (1989–2018). Icon Development Solutions, Ellicott City, MD.
33. Bjugård Nyberg H, Hooker AC, Bauer R, Aoki Y. 2017. SADDLE_RESET: more robust parameter estimation with a check for local practical identifiability, abstr 7345. Abstr Annu Meet Popul Approach Group Eur.
34. van der Graaf PH. 2014. Introduction to population pharmacokinetic/pharmacodynamic analysis with nonlinear mixed effects models. CPT Pharmacometrics Syst Pharmacol 3:e153. https://doi.org/10.1038/psp.2014.51.
35. Karlsson MO, Holford N. 2008. A tutorial on visual predictive checks, abstr 1434. Abstr Annu Meet Popul Approach Group Eur.
36. Bergstrand M, Hooker AC, Wallin JE, Karlsson MO. 2011. Prediction-corrected visual predictive checks for diagnosing nonlinear mixed-effects models. AAPS J 13:143–151. https://doi.org/10.1208/s12248-011-9255-z.
37. R Core Team. 2017. R: A language and environment for statistical computing. R Foundation for Statistical Computing, Vienna, Austria.
38. Keizer RJ, Karlsson MO, Hooker AC. 2013. Modeling and simulation workbench for NONMEM: tutorial on Pirana, PsN, and Xpose. CPT Pharmacometrics Syst Pharmacol 2:e50. https://doi.org/10.1038/psp.2013.24.
39. Beal SL. 2001. Ways to fit a PK model with some data below the quantification limit. J Pharmacokinet Pharmacodyn 28:481–504. https://doi.org/10.1023/a:1012299115260.
40. Germovsek E, Barker CIS, Sharland M, Standing JF. 2019. Pharmacokinetic-pharmacodynamic modeling in pediatric drug development, and the importance of standardized scaling of clearance. Clin Pharmacokinet 58:39–52. https://doi.org/10.1007/s40262-018-0659-0.
41. Al-Sallami HS, Goulding A, Grant A, Taylor R, Holford N, Duffull SB. 2015. Prediction of fat-free mass in children. Clin Pharmacokinet 54:1169–1178. https://doi.org/10.1007/s40262-015-0277-z.
42. WHO Multicentre Growth Reference Study Group. 2006. WHO child growth standards: length/height-for-age, weight-for-age, weight-for-length, weight-for-height and body mass index-for-age: methods and development. World Health Organization, Geneva, Switzerland.
43. de Onis M, Onyango AW, Borghi E, Siyam A, Nishida C, Siekmann J. 2007. Development of a WHO growth reference for school-aged children and adolescents. Bull World Health Organ 85:660–667. https://doi.org/10.2471/blt.07.043497.
44. Dosne A-G, Bergstrand M, Karlsson MO. 2017. An automated sampling importance resampling procedure for estimating parameter uncertainty. J Pharmacokinet Pharmacodyn 44:509–520. https://doi.org/10.1007/s10928-017-9542-0.
45. Dunne J, Rodriguez WJ, Murphy MD, Beasley BN, Burckart GJ, Filie JD, Lewis LL, Sachs HC, Sheridan PH, Starke P, Yao LP. 2011. Extrapolation of adult data and other data in pediatric drug-development programs. Pediatrics 128:e1242–e1429. https://doi.org/10.1542/peds.2010-3487.
46. Svensson EM, Yngman G, Denti P, McIlleron H, Kjellsson MC, Karlsson MO. 2018. Evidence-based design of fixed-dose combinations: principles and application to pediatric anti-tuberculosis therapy. Clin Pharmacokinet 57:591–599. https://doi.org/10.1007/s40262-017-0577-6.
47. Mattila MJ, Koskinen R, Takki S. 1968. Absorption of ethionamide and prothionamide in vitro and in vivo. Ann Med Intern Fenn 57:75–79.
48. Tiitinen H. 1969. Isoniazid and ethionamide serum levels and inactivation in Finnish subjects. Scand J Respir Dis 50:110–124.
49. Jenner PJ, Ellard GA. 1981. High-performance liquid chromatographic determination of ethionamide and prothionamide in body fluids. J Chromatogr 225:245–251. https://doi.org/10.1016/s0378-4347(00)80269-8.
50. Jenner PJ, Ellard GA, Gruer PJ, Aber VR. 1984. A comparison of the blood levels and urinary excretion of ethionamide and prothionamide in man. J Antimicrob Chemother 13:267–277. https://doi.org/10.1093/jac/13.3.267.
51. Lim T, Ding L, Zaki M, Suleiman AB, Fatimah S, Siti S, Aris T, Maimunah AH. 2000. Distribution of body weight, height and body mass index in a national sample of Malaysian adult. Med J Malaysia 55:108–128.
52. Peloquin CA, James GT, McCarthy E, Goble M. 1991. Pharmacokinetic evaluation of ethionamide suppositories. Pharmacotherapy 11:359–363.
53. Korth-Bradley JM, Mayer P, Mansfield D, Tucker H, Wu D. 2014. Comparative bioavailability study of single-dose film-coated and sugar-coated ethionamide tablets in healthy volunteers. Clin Ther 36:982–987. https://doi.org/10.1016/j.clinthera.2014.04.014.
54. Hemanth Kumar AK, Kumar A, Kannan T, Bhatia R, Agarwal D, Kumar S, Dayal R, Singh SP, Ramachandran G, Hemanth Kumar AK, Kumar A, Kannan T, Bhatia R, Agarwal D, Kumar S, Dayal R, Singh SP, Ramachandran G. 2018. Pharmacokinetics of second-line antituberculosis drugs in children with multidrug-resistant tuberculosis in India. Antimicrob Agents Chemother 62:e02410-17. https://doi.org/10.1128/AAC.02410-17.